

Exposure Time-Specific Pointing Stability Analysis for DSCOV
Michael Nemesure
November 2013

This memorandum is an addendum to an earlier memo, "Jitter and Stability Analysis for DSCOV"¹. That reference should be consulted before reading the present memorandum. The results presented previously utilized a fixed 100 ms stability window. Because the reaction wheels generally generate disturbances with frequencies greater than 10 Hz, a conservative peak-to-peak stability estimate was used throughout in the earlier analysis. Further, the controller contribution to the total stability was estimated using the 10 Hz truth model output from a standard Hifi simulation run in a nominal science mode (earth pointing, no slewing).

The present analysis incorporates actual EPIC exposure times. Based on References 2 and 3, eight stability windows corresponding to eight exposure times were analyzed. These are listed in Table 1.

EPIC Filter Channel	Exposure Time (s)
1	1.290,
2	0.840,
3	0.126,
9	0.095,
8	0.090,
4	0.087,
5	0.052,
7	0.036,
10	0.030

Table 1. Exposure Time Windows Used for Stability Analysis

As discussed in Reference 1, there are two components to the total stability: jitter-driven and controller-driven. The first arises from generally high-frequency flexing of designated points of the spacecraft relative to a rigid-body reference and is evaluated using a finite element model. The second arises from lower frequency, deviations of the rigid body from a static reference due, in part, from reaction wheel tachometer errors and gyro noise.

Incorporating Stability Windows into Jitter Stability Estimates

As Reference 1 indicates, the jitter stability is dictated by the maximum minus the minimum deviation of attitude rotation, axis-by-axis, over the sampling time τ . At a given frequency, the reaction wheel disturbances are modeled as simple sinusoids whose amplitudes are provided by the transfer functions presented in Reference 1. If the stability interval is (conservatively) centered on the steepest part of the sinusoid, the stability is $2 \sin(2\pi \tau / 4) \times$ jitter amplitude for a window of width $\tau < \pi/\omega$. For wider windows, the stability becomes $2 \times$ jitter amplitude. Figure 1 illustrates this.

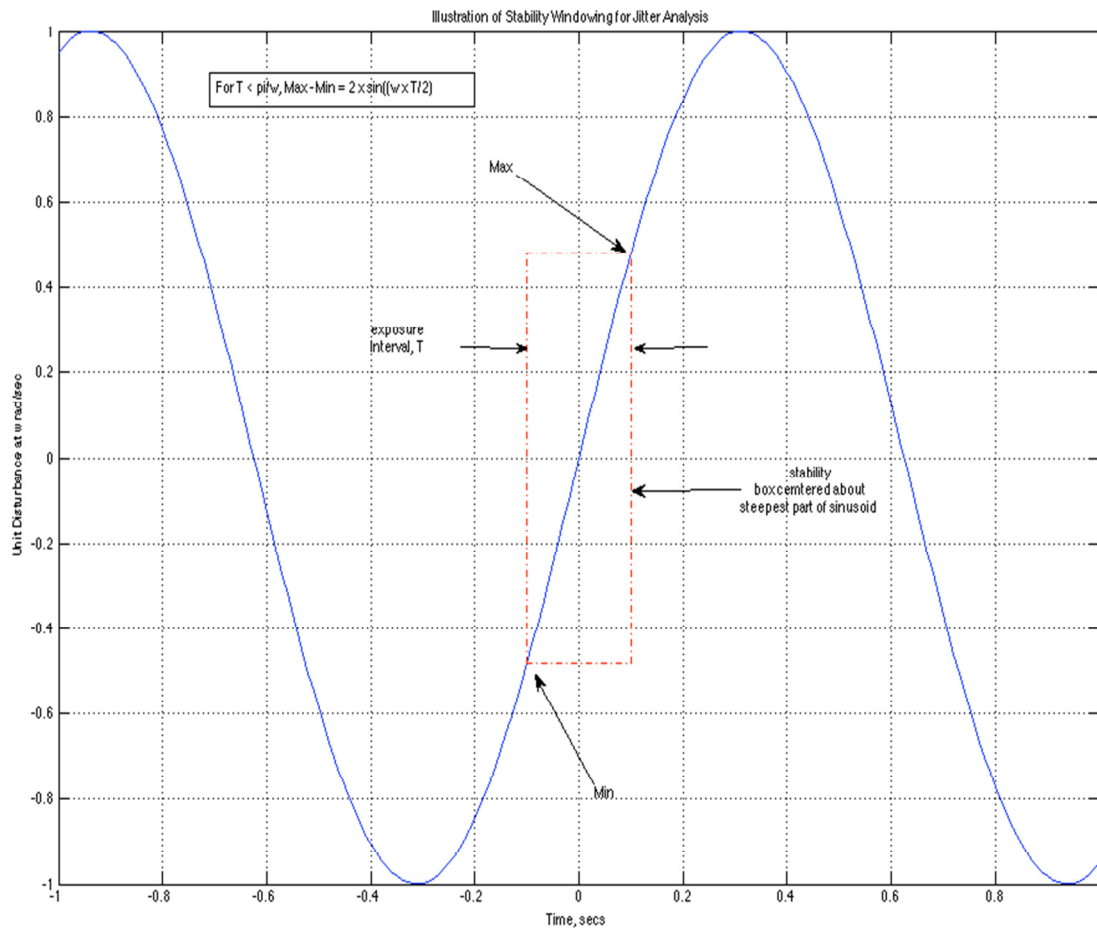


Figure 1. Illustration of Jitter Stability Window

Figure 2 shows the scale factor curves for each of the eight stability windows. When multiplied by the jitter amplitude, the scale factors provide jitter stability estimates. As can be seen, for wheel speeds above 100 rad/sec, jitter stability results for the eight exposure intervals are indistinguishable.

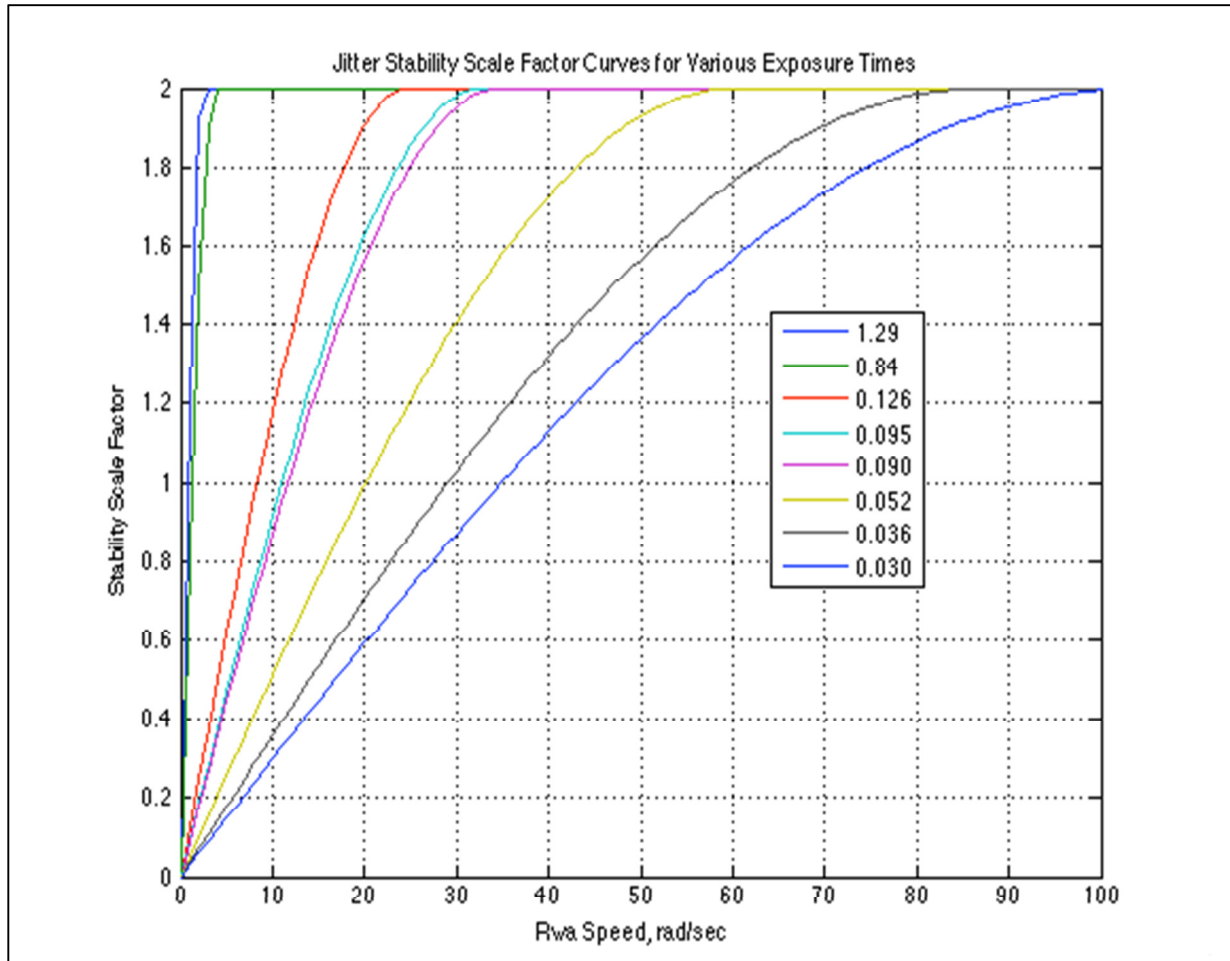


Figure 2. Jitter Stability Scale Factor Curves for Various Exposure Times

Figure 3 shows the stability results for the shortest of the windows analyzed (30 msecs) due to disturbances from each of the reaction wheels in turn. These results demonstrate that the first significant flex mode is suppressed below the requirement (horizontal dashed line in the figures) relative to earlier results. At higher frequency little change is observed.

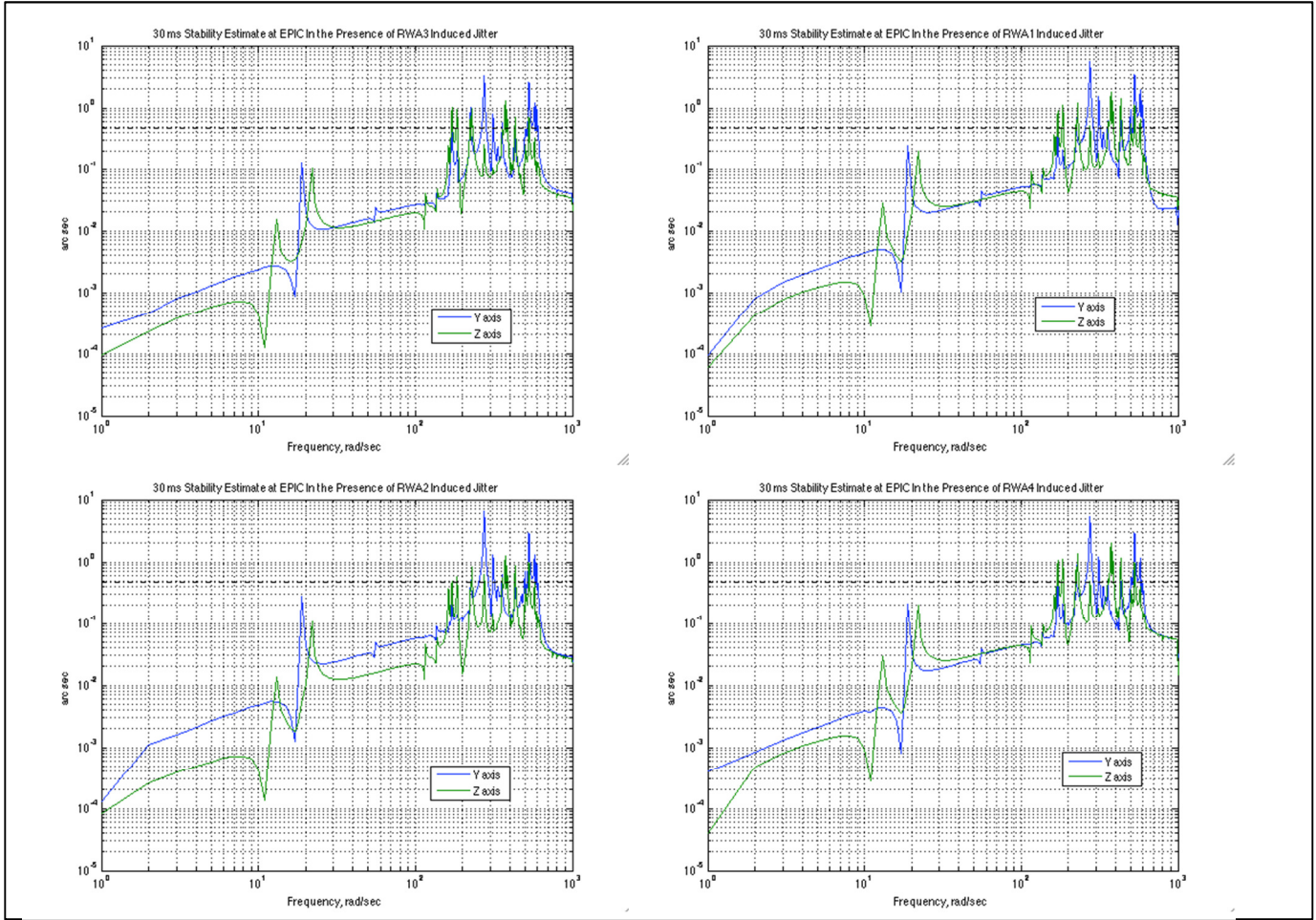


Figure 3. Jitter Stability for 30 msec Exposure Time, Reaction Wheels 1—4. Horizontal dashed lines indicate 0.47 arc sec Requirement

Incorporating Stability Windows into Controller-driven Stability Estimates

The controller-driven pointing stability is computed using a sliding window of width τ . The stability is the rms of the variation of the truth quaternion over the window.

Specifically, at time t ,

$$\delta Q_j = \begin{pmatrix} \delta x_j \\ \delta y_j \\ \delta z_j \\ \approx 2 \end{pmatrix} = 2 \times Q'_{tm_t+j*dt} \otimes Q_{tm_t}$$

where dt is the spacing between truth model output and j numbers the quaternions within the window.

The X-, Y-, and Z-axis stabilities at time t (δx , δy , and δz , respectively) are then computed as the RMS over the window starting at time t :

$$\delta x(t) = \sqrt{\frac{1}{N} \sum_{j=1}^N (0.5 \times \delta x_j)^2}$$

where $N = \tau/dt$, with similar expressions for δy and δz . The factor of 0.5 is needed to ensure that the error in increment j is not double-counted in the RMS given that it is influenced both by Q_{tm} at time t and by Q_{tm} at time $t+j*dt$;

Note that an alternative method of computing controller stability is to compute the maximum minus the minimum deviation, axis-by-axis, of the N quaternions from a fixed reference. This method would tend to produce larger stability estimates because it is skewed by variation on time scales shorter than the sampling window.

A 500-run Monte Carlo simulation was performed that randomized the system momentum within a sphere of radius 15 Nms in momentum space. The simulation target an inertial attitude, nominally with the X-axis of the SC pointed at the earth. To ensure that the stability computations above could be performed with $N > 1$ even for the shortest window, truth quaternion output was collected at 100 Hz. To avoid prohibitively large datasets, the simulation was run for only 100 seconds.

Table 2 presents the controller-driven component of pointing stability at the 99.7 percentile level.

Exposure Time, msecs	99.7 Percentile Control Stability, arc sec Y-axis	99.7 Percentile Control Stability, arc sec Z-axis
1290	4.23	3.48
840	3.00	2.51
126	0.53	0.44
95	0.42	0.34
90	0.38	0.31
52	0.26	0.22
36	0.19	0.15
30	0.15	0.12

Table 2. 3σ Control Stability Over the Final 30 seconds of a 100 second 500-run Monte Carlo Simulation with System Momentum up to 15 Nms.

Total Stability

The total stability is taken as the arithmetic sum of the controller-driven and jitter-driven stability estimates (each of which is a strictly non-negative number). As discussed previously, the rationale is that the former results from higher frequency disturbances than does the latter. This is not strictly true at the low end of the spectrum but to neglect that fact is to produce more conservative results.

The same Monte Carlo simulation was used to compute controller stability (utilizing the quaternion output) and to compute jitter stability (using reaction wheel speed output). Because the stability results are sensitive to reaction wheels speeds and, therefore, to total system momentum, separate statistics were computed for the subset of Monte Carlo runs that when no higher than 12 Nms. Tables 3 and 4 present the total stability results.

Exposure Time, msec	99.7 Percentile Total Stability, arc sec X-axis	99.7 Percentile Total Stability, arc sec Y-axis	99.7 Percentile Total Stability, arc sec Z-axis
1290.00	4.30	7.89	3.93
840.00	3.78	7.37	2.98
126.00	2.66	6.59	1.61
95.00	2.75	6.56	1.56
90.00	2.57	6.52	1.55
52.00	2.69	6.49	1.43
36.00	2.66	6.16	1.45
30.00	2.64	6.17	1.44

Table 3. 3σ Total Stability (Jitter + Controller) Over the Final 30 seconds of a 100 second 500-run Monte Carlo Simulation. System Momentum up to 15 Nms (with some RW Zero Crossings) included

WHAT IS THE FREQUENCY OF THE JITTER – DESCRIBE MOTION

Exposure Time, msec	99.7 Percentile Total Stability, arc sec X-axis	99.7 Percentile Total Stability, arc sec Y-axis	99.7 Percentile Total Stability, arc sec Z-axis
1290.00	4.00	4.19	3.57
840.00	3.76	3.06	2.99
126.00	2.78	1.37	1.53
95.00	2.77	1.15	1.54
90.00	2.65	1.13	1.54
52.00	2.77	1.09	1.42
36.00	2.74	1.07	1.45
30.00	2.74	1.05	1.45

Table 4. 3σ Total Stability (Jitter + Controller) Over the Final 30 seconds of a 100 second 390-run Monte Carlo Simulation. System Momentum up to 12 Nms (with no RW Zero Crossings) included

IS THE X-AXIS A ROTATION?

Notes and References

¹Jitter and Stability Analysis for DSCOV_R_20130821, Michael Nemesure

²EPIC TIM Max and Min Radiance, EPIC Calibration TIM, September 2010

³Expected Radiances and Exposure Times for EPIC